

## Measurements of the Generalized Electric and Magnetic Polarizabilities of the Proton at Low $Q^2$ Using the Virtual-Compton-Scattering Reaction

P. Bourgeois,<sup>1</sup> Y. Sato,<sup>2</sup> J. Shaw,<sup>1</sup> R. Alarcon,<sup>3</sup> A. M. Bernstein,<sup>4</sup> W. Bertozzi,<sup>4</sup> T. Botto,<sup>4</sup> J. Calarco,<sup>5</sup> F. Casagrande,<sup>4</sup> M. O. Distler,<sup>6</sup> K. Dow,<sup>4</sup> M. Farkondeh,<sup>4</sup> S. Georgakopoulos,<sup>7</sup> S. Gilad,<sup>4</sup> R. Hicks,<sup>1</sup> M. Holtrop,<sup>5</sup> A. Hotta,<sup>1</sup> X. Jiang,<sup>8</sup> A. Karabarbounis,<sup>7</sup> J. Kirkpatrick,<sup>5</sup> S. Kowalski,<sup>4</sup> R. Milner,<sup>4</sup> R. Miskimen,<sup>1</sup> I. Nakagawa,<sup>4,\*</sup> C. N. Papanicolas,<sup>7</sup> A. J. Sarty,<sup>9</sup> S. Sirca,<sup>4</sup> E. Six,<sup>3</sup> N. F. Sparveris,<sup>7</sup> S. Stave,<sup>4</sup> E. Stiliaris,<sup>7</sup> T. Tamae,<sup>2</sup> G. Tsentalovich,<sup>4</sup> C. Tschalaer,<sup>4</sup> W. Turchinets,<sup>4</sup> Z.-L. Zhou,<sup>4</sup> and T. Zwart<sup>4</sup>

<sup>1</sup>Department of Physics, University of Massachusetts, Amherst, Massachusetts 01003, USA

<sup>2</sup>Laboratory of Nuclear Science, Tohoku University, Mikamine, Taihaku, Sendai 982-0826, Japan

<sup>3</sup>Department of Physics and Astronomy, Arizona State University, Tempe, Arizona 85287, USA

<sup>4</sup>Department of Physics, Laboratory for Nuclear Science and Bates Linear Accelerator Center, Massachusetts Institute of Technology, Cambridge, Massachusetts 02139, USA

<sup>5</sup>Department of Physics, University of New Hampshire, Durham, New Hampshire 03824, USA

<sup>6</sup>Institute für Kernphysik, Universitaet Mainz, Mainz D-55099, Germany

<sup>7</sup>Institute of Accelerating Systems and Applications and Department of Physics, University of Athens, Athens GR-10024, Greece

<sup>8</sup>Department of Physics and Astronomy, Rutgers University, Piscataway, New Jersey 08854, USA

<sup>9</sup>Department of Astronomy and Physics, St. Mary's University, Halifax, Nova Scotia, B3H 3C3 Canada

(Received 7 April 2006; published 21 November 2006)

The mean square polarizability radii of the proton have been measured for the first time in a virtual-Compton-scattering experiment performed at the MIT-Bates out-of-plane scattering facility. Response functions and polarizabilities obtained from a dispersion analysis of the data at  $Q^2 = 0.057 \text{ GeV}^2/c^2$  are in agreement with  $O(p^3)$  heavy baryon chiral perturbation theory. The data support the dominance of mesonic effects in the polarizabilities.

DOI: 10.1103/PhysRevLett.97.212001

PACS numbers: 13.60.Fz, 13.40.Gp, 14.20.Dh

The electromagnetic polarizabilities of the nucleon provide a vital testing ground for theories of low-energy QCD and nucleon structure, and are of compelling experimental and theoretical interest [1]. In the case of atomic polarizabilities the electric polarizability is approximately equal to the atomic volume. By contrast, the electric polarizability of the nucleon is approximately  $10^4$  times smaller than the nucleon volume, demonstrating in a qualitative fashion the extreme stiffness of the nucleon relative to the atom. Although the electric and magnetic polarizabilities of the proton  $\alpha$  and  $\beta$  are known with reasonable accuracy [2] from real Compton scattering (RCS), much less is known about the polarizability distributions inside the nucleon. To measure these distributions it is necessary to use the virtual-Compton-scattering (VCS) reaction [3], where the incident photon is virtual. At low  $Q^2$  it is expected [4] that  $\alpha(Q^2)$  should decrease with increasing  $Q^2$  with a characteristic length scale given by the pion range. The first VCS experiments at Mainz [5] at  $Q^2 = 0.33 \text{ GeV}^2/c^2$  and later at Jefferson Lab (JLab) [6] at  $Q^2 = 0.92$  and  $1.76 \text{ GeV}^2/c^2$  established that  $\alpha(Q^2)$  is falling off, but with a form inconsistent with a simple dipole shape [6]. By contrast, because of the destructive interference between paramagnetism and diamagnetism which is necessary to generate a small  $\beta$ ,  $\beta(Q^2)$  is predicted [4] to be relatively flat as a function of  $Q^2$  with a 20% peaking near  $Q^2 = 0.1 \text{ GeV}^2/c^2$  caused by a paramagnetic pion-loop contribution that increases with  $Q^2$ . This Letter reports on

a VCS experiment on the proton performed at the out-of-plane scattering facility at the MIT-Bates linear accelerator at  $Q^2 = 0.057 \text{ GeV}^2/c^2$ . Data taken at this low  $Q^2$  can provide a test of chiral perturbation theory (ChPT), and are sensitive to the mean square electric and magnetic polarizability radii. At this low value of  $Q^2$  ChPT also predicts increased sensitivity to the polarizabilities  $\alpha(Q^2)$  and  $\beta(Q^2)$  relative to the Mainz kinematics [4].

The relationship between VCS cross sections and the polarizabilities is most easily seen in the low-energy expansion (LEX) of the unpolarized VCS cross section [3],

$$d^5\sigma^{\text{VCS}} = d^5\sigma^{\text{BH+Born}} + q'\Phi\Psi_0(q, \varepsilon, \theta, \phi) + O(q'^2), \quad (1)$$

where  $q$  ( $q'$ ) is the incident (final) photon three-momenta in the photon-nucleon c.m. frame,  $\varepsilon$  is the photon polarization,  $\theta$  ( $\phi$ ) is the c.m. polar (azimuthal) angle for the outgoing photon, and  $\Phi$  is a phase space factor.  $d^5\sigma^{\text{BH+Born}}$  is the cross section for the Bethe-Heitler + Born amplitudes only, i.e., no nucleon structure, and is exactly calculable from QED and the nucleon form factors. The polarizabilities enter the cross section expansion at order  $O(q')$  through the term [7]

$$\Psi_0 = V_1 \left[ P_{\text{LL}}(q) - \frac{P_{\text{TT}}(q)}{\varepsilon} \right] + V_2 P_{\text{LT}}(q), \quad (2)$$

where  $P_{\text{LL}}$ ,  $P_{\text{TT}}$ , and  $P_{\text{LT}}$  are the longitudinal, transverse,

and longitudinal-transverse VCS response functions, with  $P_{LL} \propto \alpha(Q^2)$ ,  $P_{LT} \propto \beta(Q^2)$  + spin polarizabilities, and  $P_{TT} \propto$  spin polarizabilities.  $V_1$  and  $V_2$  are kinematic functions. The Bates VCS experiment was designed to make an azimuthal separation of  $P_{LL} - P_{TT}/\varepsilon$  and  $P_{LT}$  by taking data simultaneously at  $\phi$  angles of  $90^\circ$ ,  $180^\circ$ , and  $270^\circ$ , at fixed  $\theta = 90^\circ$ . For the out-of-plane cross sections at  $\phi = 90^\circ$  and  $270^\circ$ , the cross sections are equal and the polarizability effect is proportional to  $P_{LL} - P_{TT}/\varepsilon$ . At  $\phi = 180^\circ$ , the cross section is proportional to the sum of  $P_{LL} - P_{TT}/\varepsilon$  and  $P_{LT}$ . Data were taken at five different c.m. final photon energies  $q'$  ranging from 43 MeV, where the polarizability effect is negligible, up to 115 MeV where the polarizability effect is approximately 20%. The data were taken at  $q = 240$  MeV, and  $\varepsilon = 0.9$ , corresponding to  $Q^2 \approx 0.06$  GeV<sup>2</sup>/c<sup>2</sup>. For these kinematics the sensitivities to  $\alpha(Q^2)$  in  $P_{LL} - P_{TT}/\varepsilon$  and  $\beta(Q^2)$  in  $P_{LT}$  are estimated [4] at 92% and 69%, respectively. This is to be compared with 59% and 43% at the Mainz kinematics.

The experiment was the first to use extracted beam from the MIT-Bates South Hall Ring. The extracted beams had duty factors of approximately 50%, currents of up to 7  $\mu$ A, and the five beam energies ranged from 570 to 670 MeV. The target was 1.6 cm of liquid hydrogen. The experiment marked the first use of the full Out-of-Plane Spectrometer (OOPS) system with gantry for proton detection [8], and a new One-Hundred-Inch-Proton Spectrometer (OHIPS) electron spectrometer focal plane [9] that increased the momentum acceptance of the spectrometer from 9% to 13%, giving increased acceptance in  $q'$ . Optics studies were performed to measure OHIPS transport matrix elements over the extended focal-plane instrumentation, and a new OOPS optics tune using a 2.5 m drift distance was developed for the running at  $q' = 43$  and 65 MeV because of the close packing of the OOPS's at those energies. Data taken at higher  $q'$  used the standard 1.4 m drift for the OOPS. The lowest proton kinetic energy in the experiment was 30 MeV, and the OOPS trigger was modified to a twofold trigger of the first two scintillators in the focal plane to increase trigger efficiency. A GEANT simulation of the OOPS trigger predicts a trigger efficiency of  $\approx 99\%$ . The acceptance Monte Carlo calculation was based on the program TURTLE [10], and measured spectrometer matrix elements were used for calculating focal-plane coordinates from target coordinates. The multiple scattering model [11] from GEANT4 was implemented in the acceptance Monte Carlo calculation. Good agreement was achieved between measured and calculated angular and momentum distributions.

The final state photon was identified through missing mass and time-of-flight techniques. Photon yields were obtained by fitting the missing mass squared (MM<sup>2</sup>) distributions using the radiated line shape calculated with the Monte Carlo calculation and an empirical background to account for  $A(e, e'p)X$  events on the Havar target cell wall. Polynomial and skewed Gaussian shapes for the MM<sup>2</sup> backgrounds gave identical yields within errors to fits

that used the accidental MM<sup>2</sup> distributions for the background shape, and the latter distribution was utilized for peak fitting. Radiative corrections were applied to the data [12], approximately 22% in these kinematics.

The VCS cross sections are shown in Fig. 1 with the statistical and systematic errors combined in quadrature. The dominant error is statistical, with the largest systematic uncertainty the OOPS tracking efficiency,  $\approx 1.6\%$ . The solid lines in Fig. 1 are the Bethe-Heitler + Born (BH + Born) calculations, i.e., no polarizability effect, using Hoehler form factors [13]. The agreement between data and the BH + Born calculation is good at low  $q'$ , while at higher  $q'$  the out-of-plane data falls significantly below the calculation because of destructive interference between the BH + Born and polarizability amplitudes. The in-plane cross sections show a much smaller deviation from the BH + Born cross sections at high  $q'$  because the kinematic multipliers  $V_1$  and  $V_2$  in Eq. (2) have the same sign, and therefore much of the polarizability effect is canceled at  $O(q')$ . The dashed lines in Fig. 1 are fits to the data using the LEX, giving  $P_{LL} - P_{TT}/\varepsilon = 54.5 \pm 4.8 \pm 2.0$  GeV<sup>-2</sup>, and  $P_{LT} = -20.4 \pm 2.9 \pm 0.8$  GeV<sup>-2</sup>, where the first error is statistical and the second is systematic. The largest systematic error results from the  $\pm 0.1\%$  uncertainty in the beam energies, which introduces an error in the response functions through the energy dependence of  $d^5\sigma^{\text{BH+Born}}$ . A LEX analysis using the Friedrich-Walcher form factors [14] gives identical results, within errors, to

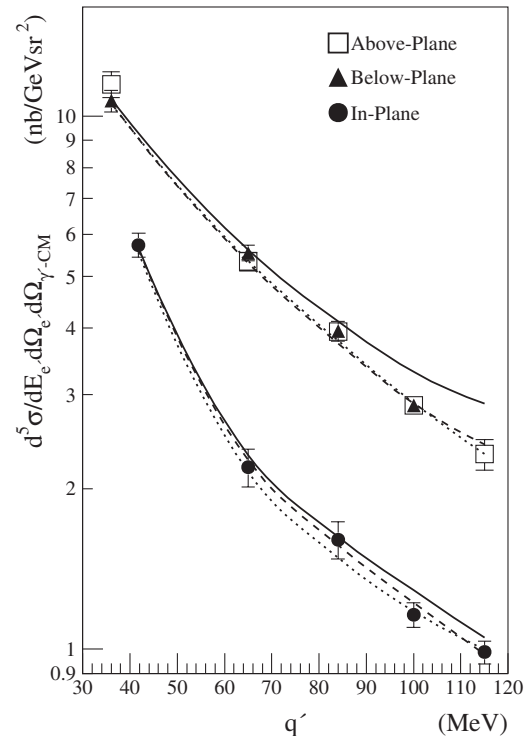


FIG. 1. VCS cross sections as a function of  $\langle q' \rangle$ . The solid curves are Bethe-Heitler + Born, the dashed and dotted curves are fits with LEX and dispersion analyses, respectively.

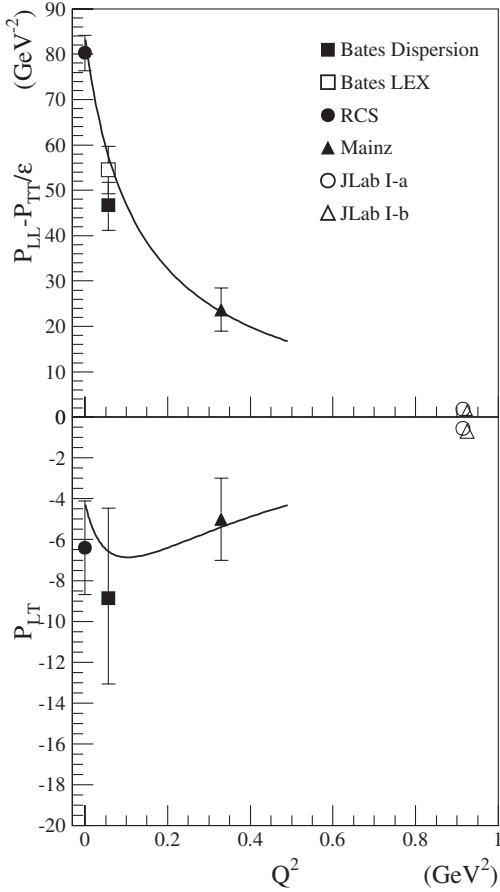


FIG. 2. VCS response functions from this experiment, RCS [2], Mainz [5], and JLab [6]. The solid curves are  $O(p^3)$  HBChPT [4].

the analysis presented here using the Hoehler form factors. The LEX result for  $P_{LL} - P_{TT}/\epsilon$  is shown in Fig. 2, where the statistical and systematic errors have been combined in quadrature. Also shown in the figure is the parameter free  $O(p^3)$  calculation in heavy baryon chiral perturbation theory (HBChPT) [4], which is in good agreement with experiment for  $P_{LL} - P_{TT}/\epsilon$ . However, the LEX result for  $P_{LT}$  (not shown in Fig. 2) is much larger than the RCS result and the HBChPT prediction.

A dispersion analysis of the data was performed using the VCS dispersion model [15]. In this analysis the VCS amplitudes are obtained from the MAID  $\gamma * p \rightarrow N\pi$  multipoles [16], and the unconstrained asymptotic contributions to 2 out of the 12 VCS amplitudes are varied to fit the VCS data. The dotted curves in Fig. 1 show the best dispersion fits to the VCS cross sections. The polarizabilities are found by summing the fitted asymptotic terms with calculated  $\pi N$  dispersive contributions, and  $P_{LL} - P_{TT}/\epsilon$  and  $P_{LT}$  are obtained from  $\alpha$ ,  $\beta$  and spin polarizabilities calculated in the dispersion model. The best fit response functions from the dispersion analysis are  $P_{LL} - P_{TT}/\epsilon = 46.7 \pm 4.9 \pm 2.0 \text{ GeV}^{-2}$  and  $P_{LT} = -8.9 \pm 4.2 \pm 0.8 \text{ GeV}^{-2}$ . The dispersion results are shown in Fig. 2 with the statistical and systematic errors combined in

quadrature. The dispersion result for  $P_{LL} - P_{TT}/\epsilon$  is in near agreement with the LEX analysis and the HBChPT predictions. The dispersion result for  $P_{LT}$  is in good agreement with the HBChPT prediction, and is much smaller than the LEX result.

The source of disagreement between the LEX and dispersion analyses for  $P_{LT}$  is the near cancellation of the electric and magnetic polarizability responses at  $O(q')$  for the in-plane kinematics, causing the polarizability effect to be predominantly quadratic in  $q'$ . The LEX analysis is only valid in kinematics where the polarizability effect is linear in  $q'$  [see Eq. (1)], while the dispersion analysis is valid to all orders in  $q'$  [17].

The dispersion model fits give  $\alpha = 7.85 \pm 0.87 \pm 0.36 \times 10^{-4} \text{ fm}^3$  and  $\beta = 2.69 \pm 1.48 \pm 0.28 \times 10^{-4} \text{ fm}^3$ , and these results are shown in Fig. 3 with the statistical and systematic errors combined in quadrature, along with previous results from RCS [2], Mainz [18], and JLab [6]. The Bates results for  $\alpha$  and  $\beta$  are in near agreement with the HBChPT prediction, shown as the solid curves in Fig. 3. Taken as a group, the  $\beta(Q^2)$  data below  $Q^2 = 0.4 \text{ GeV}^2/c^2$  suggests a flat or nearly flat magnetic response as a function of  $Q^2$ , in agreement with the

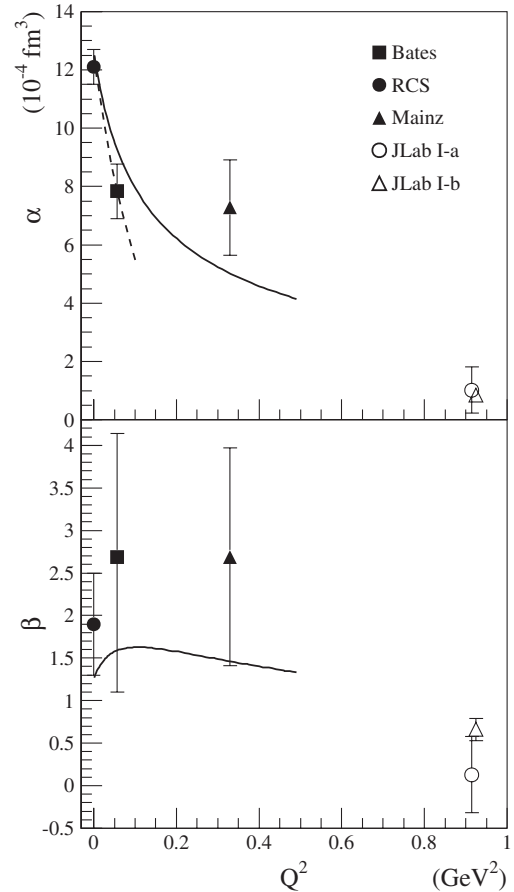


FIG. 3. Dispersion analysis results for  $\alpha(Q^2)$  and  $\beta(Q^2)$ . The references are the same as in Fig. 2 except for Mainz [18]. The solid curves are  $O(p^3)$  HBChPT [4], the dashed curve is a low  $Q^2$  fit to  $\alpha(Q^2)$ .

TABLE I. Response function units are  $\text{GeV}^{-2}$ , the polarizabilities  $10^{-4} \text{ fm}^3$ , and the mean square radius  $\text{fm}^2$ . The errors are statistical and systematic, respectively.

	LEX analysis	Dispersion analysis	HBChPT [4]
$P_{\text{LL}} - P_{\text{TT}}/\varepsilon$	$54.5 \pm 4.8 \pm 2.0$	$46.7 \pm 4.9 \pm 2.0$	56.9
$P_{\text{LT}}$	-	$-8.9 \pm 4.2 \pm 0.8$	-6.5
$\alpha(Q^2 = 0.057)$	-	$7.85 \pm 0.87 \pm 0.36$	9.27
$\beta(Q^2 = 0.057)$	-	$2.69 \pm 1.48 \pm 0.28$	1.59
$\langle r_\alpha^2 \rangle$	-	$2.16 \pm 0.31$	1.7

HBChPT prediction. The theoretical errors [19] for  $\alpha(Q^2)$  and  $\beta(Q^2)$  at  $Q^2 = 0.06 \text{ GeV}^2/c^2$  are estimated to be comparable to the errors for an  $O(p^4)$  calculation [20] of  $\alpha$  and  $\beta$ , approximately  $\pm 2.0$  and  $\pm 3.6$  in units of  $10^{-4} \text{ fm}^3$ , respectively.

The mean square electric polarizability radius  $\langle r_\alpha^2 \rangle$  was determined from a HBChPT fit to the RCS and Bates  $\alpha(Q^2)$  data points, where the  $O(Q^2)$  term in the momentum expansion of the HBChPT prediction was varied to fit the data. The fit gives  $\langle r_\alpha^2 \rangle = 2.16 \pm 0.31 \text{ fm}^2$ , which is in near agreement with the HBChPT prediction [21] of  $1.7 \text{ fm}^2$ . The experimental value is significantly larger than the proton mean square charge radius [22] of  $0.757 \pm .014 \text{ fm}^2$ , which is evidence for the dominance of mesonic effects in the electric polarizability. It is interesting to note that the experimental result is close to the uncertainty principle estimate of  $2.0 \text{ fm}^2$  for the size of the pion cloud.

The experimental results are summarized in Table I. The experiment supports two long-accepted, although arguably not fully tested, tenets of the proton polarizability. The first is that the electric polarizability is dominated by mesonic effects, and this is confirmed by the size of  $\langle r_\alpha^2 \rangle$ . The second is the cancellation of positive paramagnetism by negative diamagnetism, a critical element in explanations for the small size of  $\beta$  relative to  $\alpha$ , and evidence for this is suggested by the relative flatness of the  $\beta(Q^2)$  data at low  $Q^2$ .

Future developments in this field can be expected from VCS measurements of the proton spin polarizabilities at Mainz [23] utilizing polarized beam and recoil polarimetry. RCS experiments at TUNL/HIGS [24] will utilize polarized beam and targets to measure the four spin polarizabilities of the nucleon, three of which are related to the VCS generalized polarizabilities [4] in the limit  $q \rightarrow 0$ , as well as making precision measurements of  $\beta$ .

The authors thank T. Hemmert, B. Holstein, I. L'vov, B. Pasquini, and M. Vanderhaeghen for their comments and for communicating the results of their calculations. The authors also thank the staff of the MIT-Bates linear accelerator facility for their efforts on this experiment. This work was supported in part by the program Pithagoras of the Hellenic Ministry of Education, by Grant-in-Aid for Scientific Research from the Japan Society for the Promotion of Science (KAKENHI, Grants No. 14540239 and No. 17540229), and by D.O.E. Grant No. DE-FG02-88ER40415.

\*Present address: RIKEN, Wako, Saitama 351-0198, Japan.

- [1] B. Holstein, Comments Nucl. Part. Phys. **19**, 221 (1990).
- [2] M. Schumacher, Prog. Part. Nucl. Phys. **55**, 567 (2005).
- [3] P. A. M. Guichon *et al.*, Nucl. Phys. **A591**, 606 (1995).
- [4] T. R. Hemmert *et al.*, Phys. Rev. Lett. **79**, 22 (1997); T. R. Hemmert *et al.*, Phys. Rev. D **62**, 014013 (2000).
- [5] J. Roche *et al.*, Phys. Rev. Lett. **85**, 708 (2000).
- [6] G. Laveissiere *et al.*, Phys. Rev. Lett. **93**, 122001 (2004).
- [7] P. A. M. Guichon and M. Vanderhaeghen, Prog. Part. Nucl. Phys. **41**, 125 (1998).
- [8] S. Dolfini *et al.*, Nucl. Instrum. Methods Phys. Res., Sect. A **344**, 571 (1994); J. Mandeville *et al.*, Nucl. Instrum. Methods Phys. Res., Sect. A **344**, 583 (1994); Z. Zhou *et al.*, Nucl. Instrum. Methods Phys. Res., Sect. A **487**, 365 (2002).
- [9] X. Jiang, Ph.D. thesis, University of Massachusetts, 1998 (unpublished).
- [10] Fermi National Accelerator Laboratory Report No. NAL-64, 1978.
- [11] H. W. Lewis, Phys. Rev. **78**, 526 (1950).
- [12] M. Vanderhaeghen *et al.*, Phys. Rev. C **62**, 025501 (2000).
- [13] G. Hoehler, E. Pietarinen, and I. Sabba-Stefanescu, Nucl. Phys. **B114**, 505 (1976).
- [14] J. Friedrich and Th. Walcher, Eur. Phys. J. A **17**, 607 (2003).
- [15] B. Pasquini *et al.*, Eur. Phys. J. A **11**, 185 (2001); D. Drechsel, B. Pasquini, and M. Vanderhaeghen, Phys. Rep. **378**, 99 (2003).
- [16] D. Drechsel, O. Hanstein, S. S. Kamalov, and L. Tiator, Nucl. Phys. **A645**, 145 (1999).
- [17] B. Pasquini and M. Vanderhaeghen (private communication).
- [18] H. Fonvieille, and also Fig. 2 of Ref. [6] (private communication).
- [19] B. Holstein (private communication).
- [20] V. Bernard, N. Kaiser, A. Schmidt, and Ulf-G. Meißner, Phys. Lett. B **319**, 269 (1993); V. Bernard, N. Kaiser, Ulf-G. Meißner, and A. Schmidt, Z. Phys. A **348**, 317 (1994).
- [21] T. R. Hemmert, B. R. Holstein, G. Knochlein, and S. Scherer, Phys. Rev. D **55**, 2630 (1997).
- [22] S. Eidelman *et al.*, Phys. Lett. B **592**, 1 (2004).
- [23] Mainz experiment A1/1-00, N. D'Hose and H. Merkel spokespersons.
- [24] M. Ahmed *et al.*, "Compton Scattering on Nucleon and Nuclear Targets," TUNL 2005 (unpublished).